

4.4 Injector Linear Accelerator

100 MeV S-band linear accelerator based on the components already built for the S-Band Linear Collider Test Facility at DESY [1, 2] will be used as an injector for the CANDLE booster ring. The linac design and layout will fulfill the following basic requirements:

- Single, multi-bunch and top-up injection operation modes;
- Nominal repetition rate 2 Hz;
- Energy spread in single pulse 0.5%;
- Pulse-to-pulse energy spread of 0.25%;
- The current injection rate at 100 MeV – 400 mA/min;
- Minimum beam losses.

The general scheme of injector complex is shown in Fig. 4.4.1.

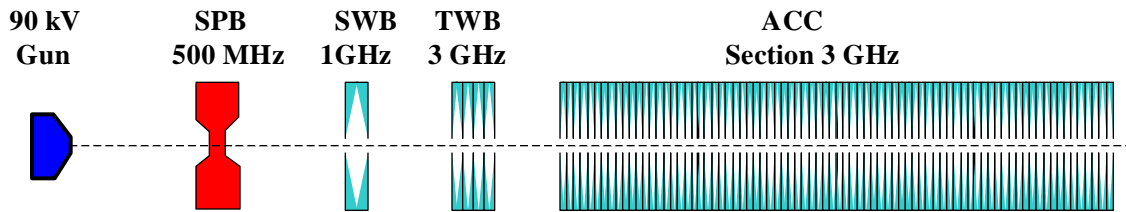


Fig. 4.4.1. The schematic layout of injector linac.

The maximum duration of the single bunch at the electron gun exit is 1 ns with 1.6 nC charge ($\sim 10^{10}$ electrons, peak current 2.2 A), while the maximum duration of the bunch train for multi-bunch operation mode is 600 nsec with maximum total charge of 6 nC (10 mA pulse current).

An electron pulse from the gun modulated by 500 MHz amplifier is captured by sequentially located 500 MHz sub-harmonic pre-buncher (SPB), 1 GHz pre-buncher cavity and 3 GHz traveling wave (TW) structure. The result is the 500 MHz pulse structure with more than 90% of beam captured in 20° of 3 GHz phase duration.

In multi-bunch operation mode, a 480 ns long electron pulse from the linac will fill the 240 RF buckets of the booster, out of possible 320 (at 499.476 MHz). This will leave 160 nsec for the injection kicker field to decay before the beam reaches the injection point on its second pass. The injection energy to booster of 100 MeV corresponds to an injection field of 24 mT in the booster, and is high enough to reduce the difficulties due to tune change during the booster ramp.

The whole linac (Fig. 4.4.1) consists of gun equipment (0.7 m), drift (0.43 m), 500 MHz buncher, the second drift (~ 0.15 m), the 1 GHz buncher (~ 0.1 m), third drift (~ 0.1 m), a 3 GHz TW buncher (0.08 m). After 0.6 m of drift, the beam enters to the 6 m accelerating section with the gradient of 17 MeV/m. The drift spaces are equipped with the correction coils, focusing solenoids, beam position monitors (BPM) and the screens (or wires) for beam profile detection.

4.4.1 Electron Gun

The gun is the standard triode gun, modulated by 500 MHz amplifier, which matches the beam pulse structure already at the gun to the booster and storage ring RF-bucket structure avoiding the beam losses at high energy in the booster ring. The result is a gun pulse with a length of ~ 1 nsec.

The voltage between the gun cathode and anode is 90 kV. Two operating modes are considered with the pulse length of 1ns (single bunch mode) and 200-600ns (multi-bunch mode) according to linac specification. In the single bunch mode the cathode is pulsed with respect to grid. In the multi-bunch mode the grid is modulated at 500 MHz with respect to the cathode. The cathode is a standard EIMAC YU-171 with the radius of 5.6 mm and emission surface of ~ 1 cm². The main characteristics of the gun performance are given in Table 4.4.1.

Table 4.4.1. The main characteristics of 90kV triode gun for CANDLE.

Parameters	Single bunch mode	Multi bunch mode
Cathode (YU-171) radius (mm)	5.6	5.6
Cathode-anode distance (mm)	35	35
Electron bunch length (ns)	1	200-600
Transverse beamsize at gun exit (mm)	6.6	4.8
Emittance at gun exit $\epsilon_{x \text{ norm}}$ (mm-mrad)	10π	10.25π
Maximum electron current (mA)	1500	15
Electron energy (keV)	90	90
Average Current Density (mA / μ m ²)	20	0.3

The electron emission from cathode has been simulated by E-GUN code [3]. Fig. 4.4.2 shows the current flow in the gun section for the maximum electron current of 1.5 A (single bunch mode) and 15 mA (multi-bunch mode). The normalized emittances of the electron beam at the gun exit are 10 and 10.25π mm·mrad for single and multi-bunch operation modes respectively.

In multi-bunch operation mode at the gun exit the 90 keV electron beam has a natural emittance of 16π mm·mrad. With the transverse beam size (3σ) of 4.8 mm this corresponds to the Twiss parameters $\alpha = 0$, $\beta = 14.4$ cm. The output pulse full width is expected to be 1.2 ns with about 90% of particles located in FWHM length of 1 ns. The 90 keV gun pulse is guided by the 40 Gauss solenoidal magnetic field along the distance of 0.7 m. This section is also equipped by correction coils, beam position monitor, valve and pumping port. Fig. 4.4.3 shows the current density at the cathode surface and Fig. 4.4.4 shows the transverse beam phase space of the beam at the cathode output.

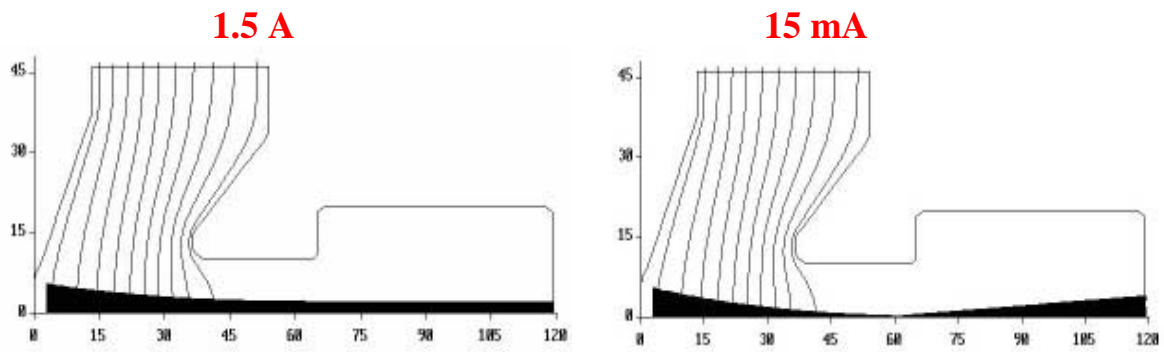


Fig. 4.4.2 The electrons flow in the gun with cathode radius of 5.6mm.

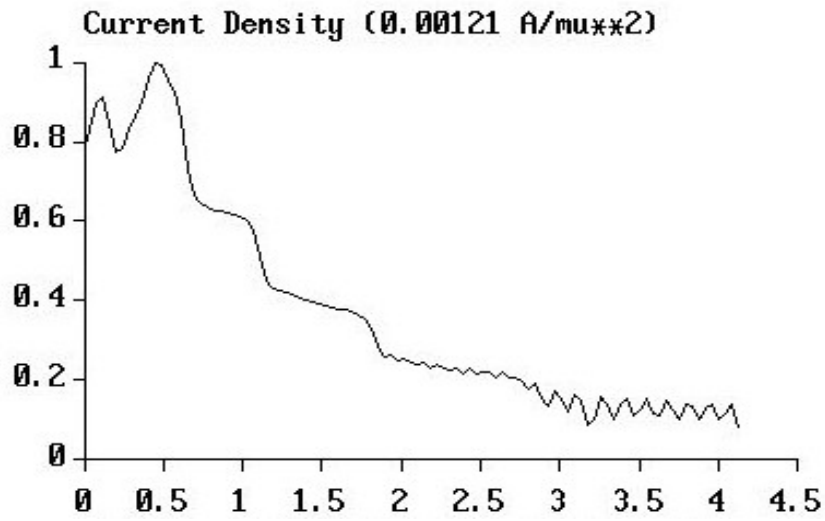


Fig. 4.4.3 Current density at cathode surface.

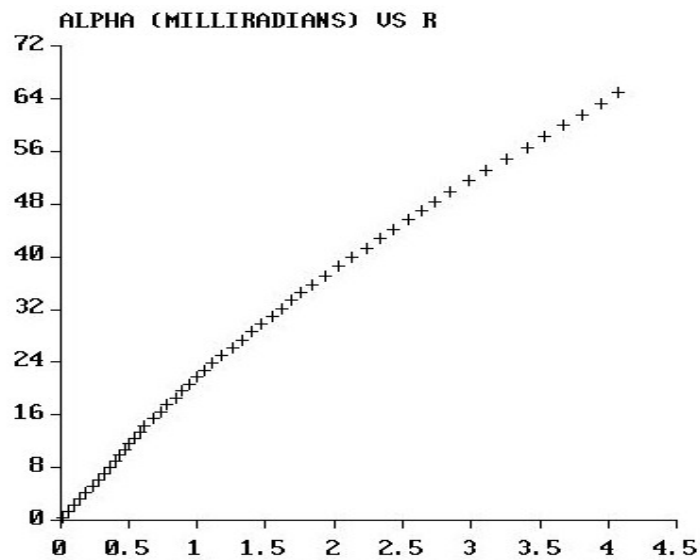


Fig. 4.4.4 The beam phase space in cylindrical coordinates at gun exit.

4.4.2 Bunching Section

The bunching section of the pre-injector consists of a 500 MHz sub-harmonic pre-buncher cavity (SPB), 1 GHz pre-buncher cavity (16 keV) and 3 GHz travelling wave structure. The SPB that is similar to buncher cavity designed for the SBLC test facility is located at the distance of 0.43 m behind the gun and compresses the 1 ns gun pulse to smaller rms length. In order to perform an effective velocity modulation along the pulse, the SPB cavity voltage is optimised to 30 kV across the buncher gap. The parameter list of the buncher cavity is given in Table 4.4.2.

Table 4.4.2 Parameter list of SPB cavity.

Gap aperture diameter (mm)	34
Gap length (mm)	40
Overall length (mm)	200
Diameter of cavity (mm)	350
Material	Stainless steel
RF wavelength (cm)	60
Shunt impedance R (MΩ)	0.27
Q – value	2700
Voltage (kV)	30

The 6 dimensional phase space of the beam has been tracked along the bunching system. Fig. 4.4.5 shows the beam distribution at the gun exit that is taken as an input for PARMELA code simulation [4]. The initial beam shape is given by the elliptical distribution in three directions: longitudinal, horizontal and vertical. The longitudinal phase is expanded within the $-600 \div +600$ degree of 3 GHz structure that corresponds to particle longitudinal distribution of 1.2 nsec. The SPB is located at the distance 43 cm and performs the bunching of the electron beam. Fig. 4.4.5 shows the beam distribution at the 500 MHz buncher entrance.

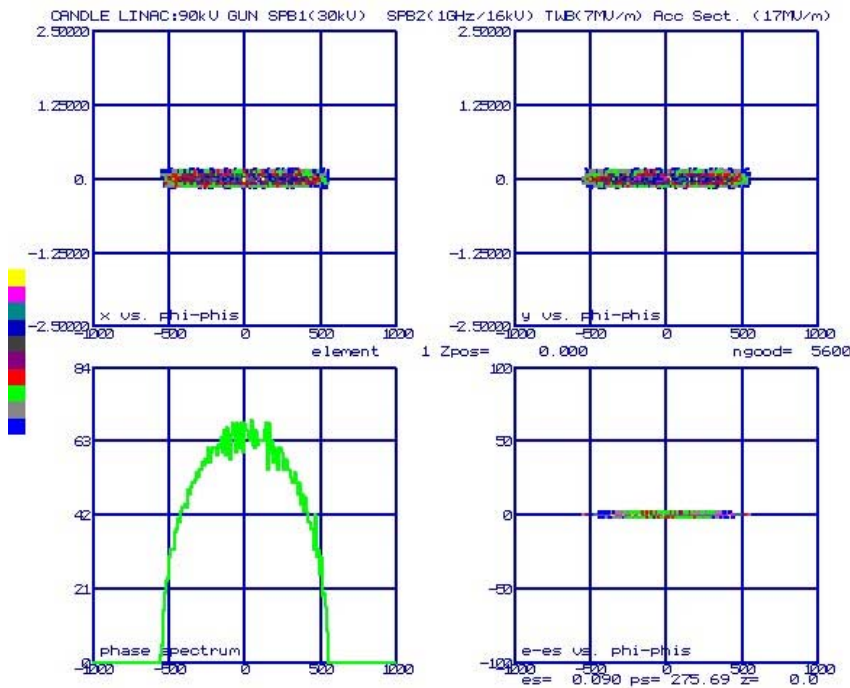


Fig. 4.4.5 Particle distributions at the 500 MHz SPB entrance a) x vs phase, b) y vs phase, c) number of particles vs phase, d) energy spread vs phase.

The optimal bunching performance [5] of the beam is achieved at the distance of

$$L_{bunching} = \frac{\lambda_{RF}}{2\pi} \frac{m_e c^2 \beta^3 \gamma^3}{eU_{peak}}, \quad (4.4.1)$$

where λ_{RF} is the cavity RF wavelength, $m_e c^2$ is the rest energy of electrons, $\beta = v/c$, γ is the particle Lorentz factor, e is the electron charge, U_{peak} is the peak cavity gap voltage. With given parameters for the gun and SPB the optimal bunching is achieved at a distance of about 35 cm following a 500 MHz buncher. This is accomplished by having a significant proper velocity modulation with the positive energy-phase correlation of the particles so that the head particles are slower and the tail particles are faster. At the optimal bunching position, the energy-phase correlation still should have the positive slope therefore the optimal distance after the buncher has been found to be 29 cm. Fig. 4.4.6 presents the longitudinal beam distribution just after the buncher and at the distance of 29 cm after beam passes the buncher cavity.

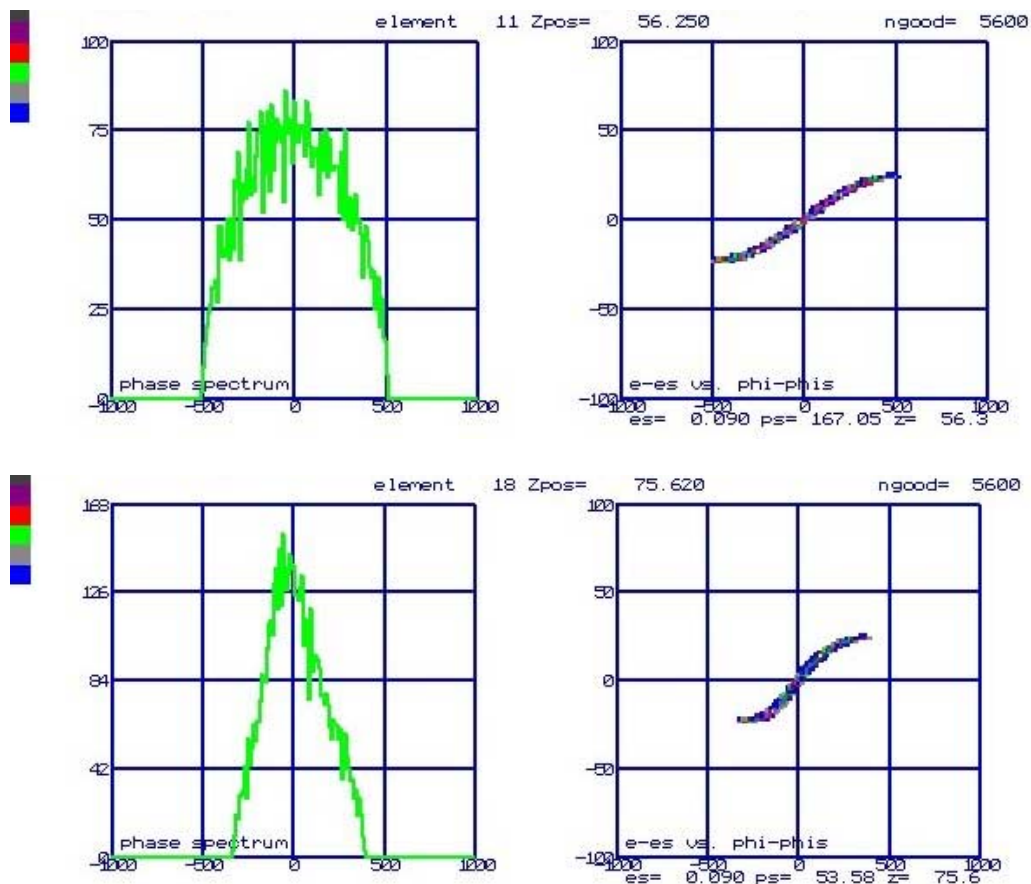


Fig. 4.4.6 The beam longitudinal distribution at the 500MHz buncher exit (top) and at the distance 29 cm after the buncher (bottom).

The 30 kV amplitude voltage of SPB cavity provides the capture of about 50% of particles within 30° of 3GHz pulse structure. The power needed to create 30 kV voltage across the gap is 1.6 kW.

After the 500 MHz SPB cavity, the compressed 90 keV energy beam with more than 70% charge in one 3 GHz wavelength (10 cm) enters into 1 GHz bunching cavity with the peak voltage of 16 kV. Actually, the second 1 GHz buncher constitutes the second harmonic of

the optimal linear voltage needed for the effective bunching. The buncher cavities do not change the kinetic energy of the bunch, which is still defined by the gun voltage of 90 kV that corresponds to velocity $\beta = v/c = 0.526$. As the direct acceleration of such a non-relativistic beam in $\beta = 1$ phase velocity, the main S-Band structure leads to a large energy spread of about 5%. One 3 GHz traveling wave (TW) structure is used for pre-acceleration and bunching purpose before beam enters into the main linac structure. The 3 GHz TW section is located at the distance of 10 cm after 1 GHz buncher cavity. This is a $2\pi/3$ mode structure with a phase velocity of $0.6c$ and a length of 8 cm (4 cells). The input RF power is 3 MW and the gradient 4 MV/m. Fig. 4.4.7 shows the beam longitudinal distribution after the 1 GHz buncher cavity and at the 3 GHz TW structure entrance.

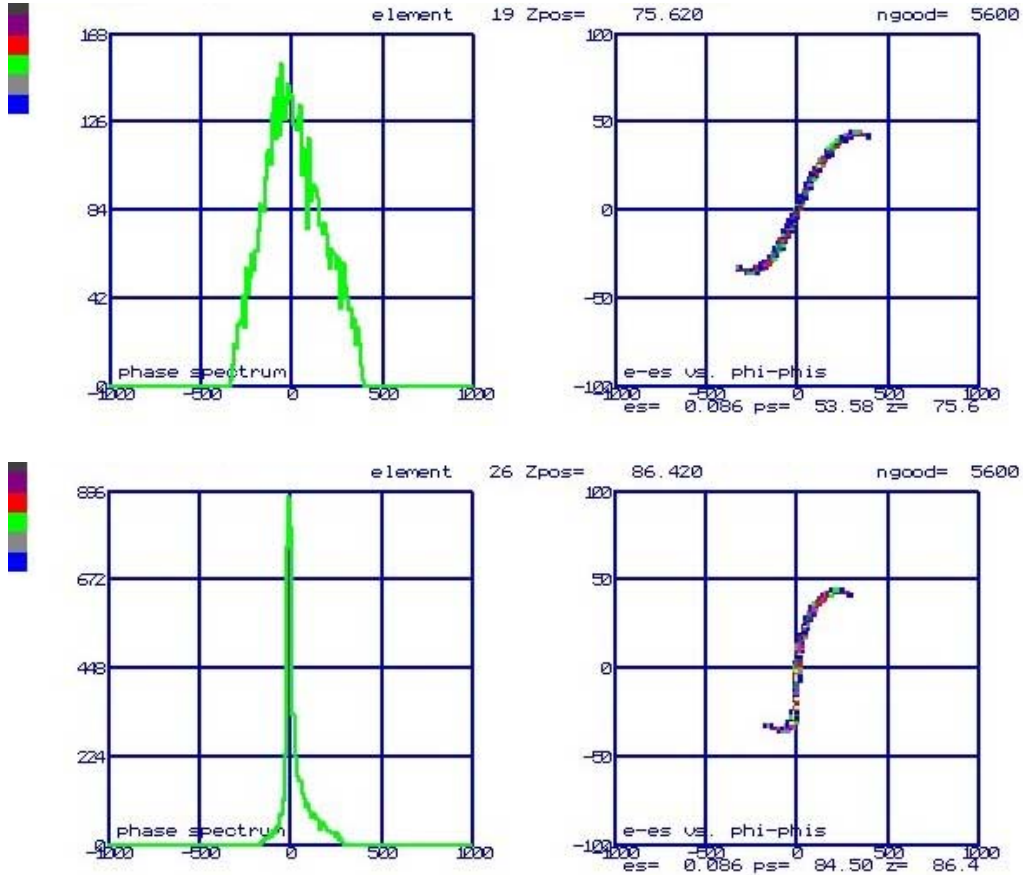
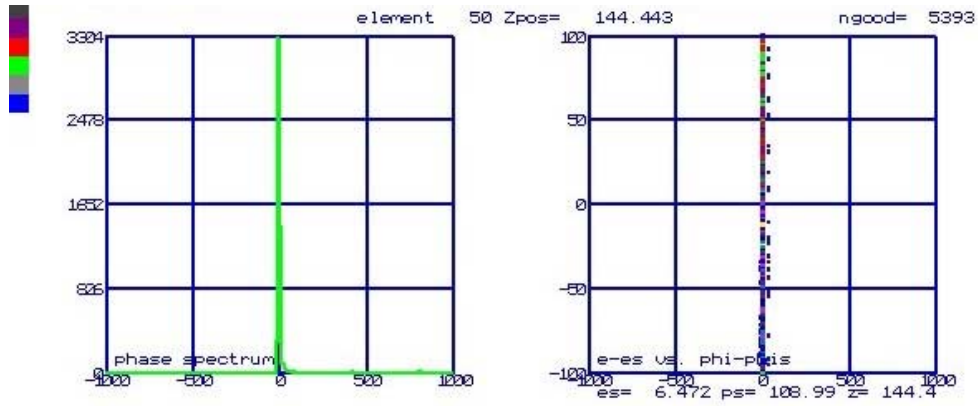


Fig. 4.4.7 Longitudinal distribution after 1 GHz buncher cavity (top) and at the 3 GHz TW structure entrance (bottom).

The bunching system provides the capture of more than 90% particles by the main 3 GHz linac section with the 17 MeV/m. The final stable longitudinal particle distribution in main linac accelerating section is shown in Fig. 4.4.8 (top), which contains more than 90% of particles in about 18° of 3 GHz structure. Fig. 4.4.8 (bottom) gives the number of the transmitted particles along the bunching section. From the initial 5600 tracked particles, only 220 particles have been lost during the whole bunching and pre-acceleration, which is about 4% of the beam loss. The beam normalized rms transverse emittances along the pre-injector are given in Fig. 4.4.9.



Beam Transmission

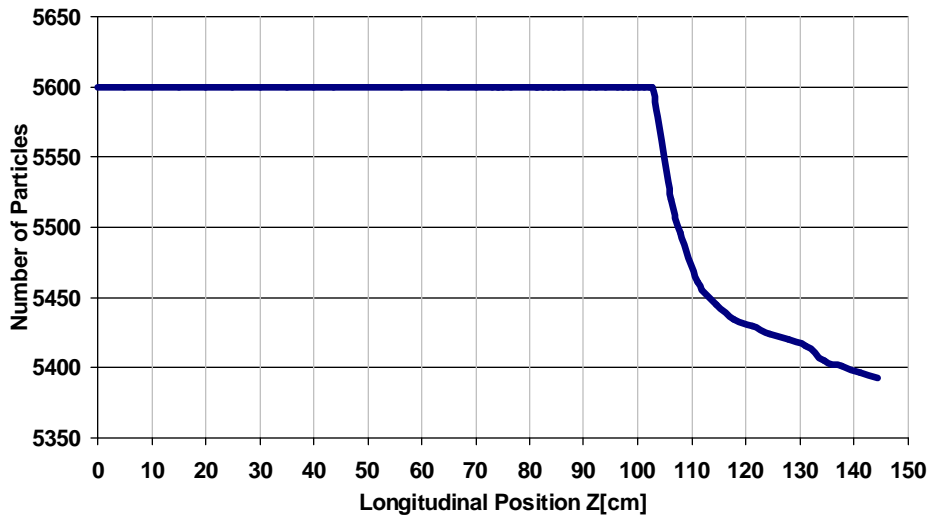


Fig. 4.4.8 The stable longitudinal beam distribution in main accelerating section (top) and beam transmission versus beam position (bottom).

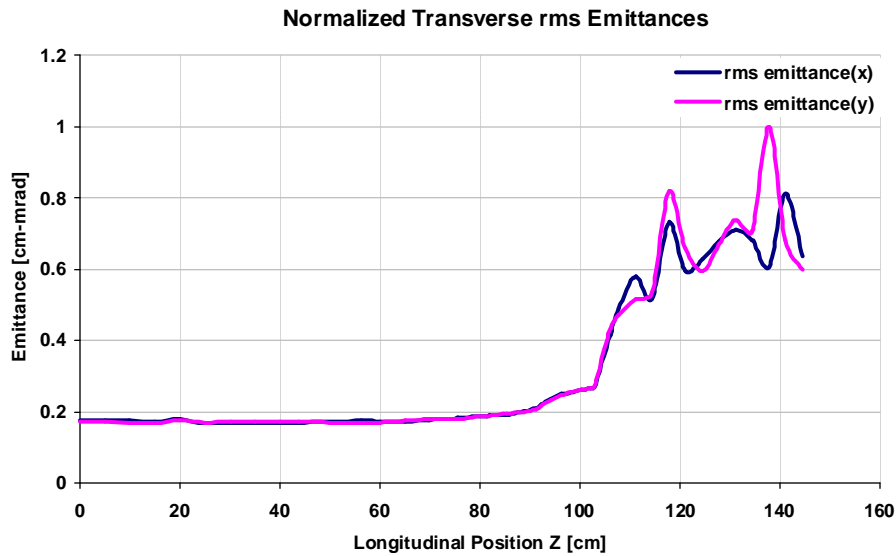


Fig. 4.4.9 The beam normalized transverse rms emittances versus beam position.

4.4.3 The 100 MeV Linac

The output current for 500 ns long electron pulse is given by the demand to fill the CANDLE storage ring within one minute to a mean current of 350 mA. Taking into account the booster synchrotron repetition rate of 2 Hz and the revolution time of 720 ns in CANDLE storage ring one gets:

$$I = \frac{350mA \cdot 720nsec}{60sec \cdot 2sec^{-1} \cdot 500nsec} = 4.2mA. \quad (4.4.2)$$

Considering some losses in the whole injection chain, a linac output current of 15 mA will be more than sufficient. With one standard 6 m long accelerating section, developed for SBLC Test Facility at DESY, the 100 MeV energy is reached by beam loaded accelerating gradient of about 17 MV/m. The structure is the constant gradient type. The parameters of the linac accelerating section are presented in Table 4.4.3.

Table 4.4.3 Parameters of the SBLC accelerating section.

Acc. Section Parameters	SBLC
Section length, L (m)	6
Attenuation, τ (neper)	0.55
Group velocity variation, v_g % of c	4.1-1.3
Filling time, T_f (nsec)	790
Shunt impedance variation, R ($M\Omega/m$)	45-61
Number of cells	180

The unloaded energy gain V_0 of a constant gradient section, ignoring the weak variation of shunt impedance R along the structure, is given by:

$$V_0^2 = RLP_0(1 - e^{-2\tau}), \quad (4.4.3)$$

where P_0 is the input power to the structure, τ is the attenuation parameter, R is the average shunt impedance per unit length, L is the structure length.

The voltage V_b , induced by the beam current of I_0 in the structure, results in the energy loss by beam and is given by:

$$V_b = I_0RL \cdot [0.5 - e^{-2\tau}(1 - e^{-2})^{-1}]. \quad (4.4.4)$$

The net voltage gain in a beam-loaded structure is then $V = V_0 \cos\theta - V_b$, where θ is the phase of the current bunches with respect to the crest of the generator produced wave. Table 4.4.4 represents the RF power requirements for the linac.

Table 4.4.4 RF Power requirements.

Parameters	SBLC Structure
Average shunt impedance R_{av} ($M\Omega$)	53
Beam loading voltage, V_b (MV)	1.9
Voltage gain in structure (MV)	100
Acceleration Gradient, U (MV/m)	17
Input power, P_0 (MW)	48
Power dissipated in the structure, P_w (MW)	31
Power to beam P_b (MW)	5
Power at the output of the structure P_L (MW)	12
Efficiency P_b/P_0 (%)	10.4

The accelerating section will be powered by 150 MW S-band klystron developed for the SBLC project in collaboration of SLAC, TU-Darmstadt and DESY. The tube is complete, and has been tested at DESY test facility. The klystron reached 150 MW at 3 μ sec pulse duration with repetition rate of 50 Hz. 150 MW S-band klystron parameters are given in Table 4.4.5. Fig. 4.4.10 presents the longitudinal and transverse particle distributions at the exit of 100 MeV injector linac.

Table 4.4.5 Klystron parameter

	SBLC (Tube 2)
Power Out	150 MW
Pulse duration	3 μ sec
Repetition rate	60 Hz
Average power	27 kW
Beam Voltage	508 kV
Beam current	652 A
Efficiency	45%

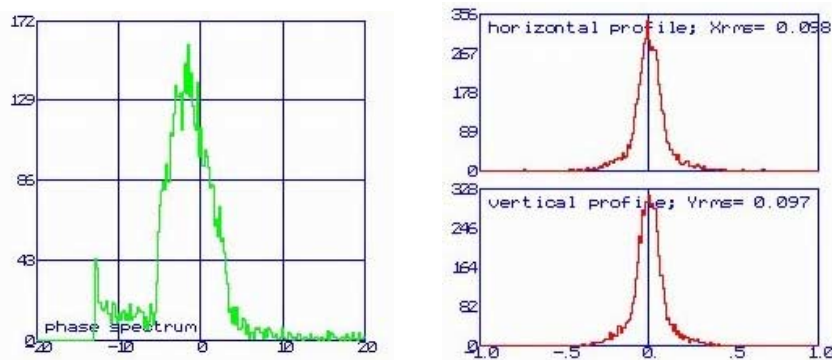


Fig. 4.4.10 Longitudinal and transverse particle distributions at the linac exit.

More than 90% of beam is transmitted through the linac and captured in 15° of the 3 GHz RF structure (Fig. 4.4.10, left). The number of transmitted particles along the whole linear injector complex is given in Fig. 4.4.11. The transverse normalized emittance evaluation along the whole linac (top) and the phase plane distributions of accelerated beam (bottom) are given in Fig. 4.4.12.

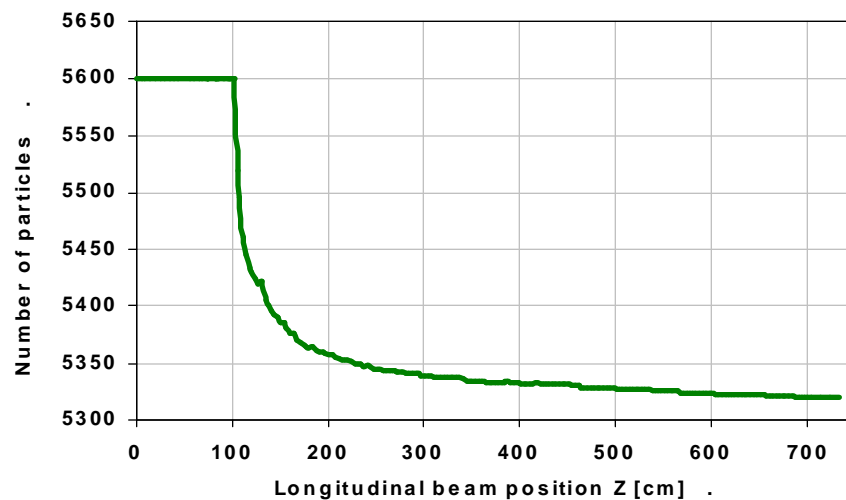


Fig. 4.4.11 Particles transmission along the whole linac.

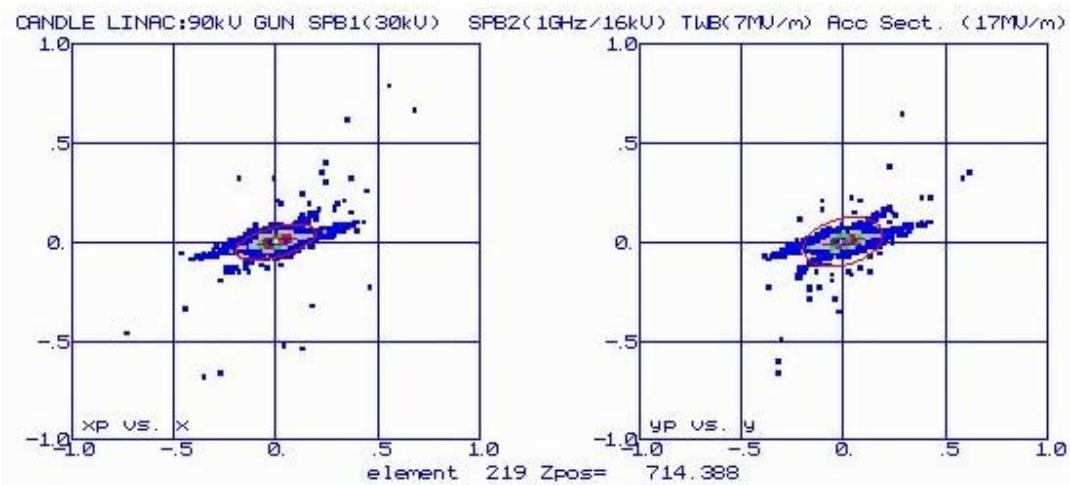
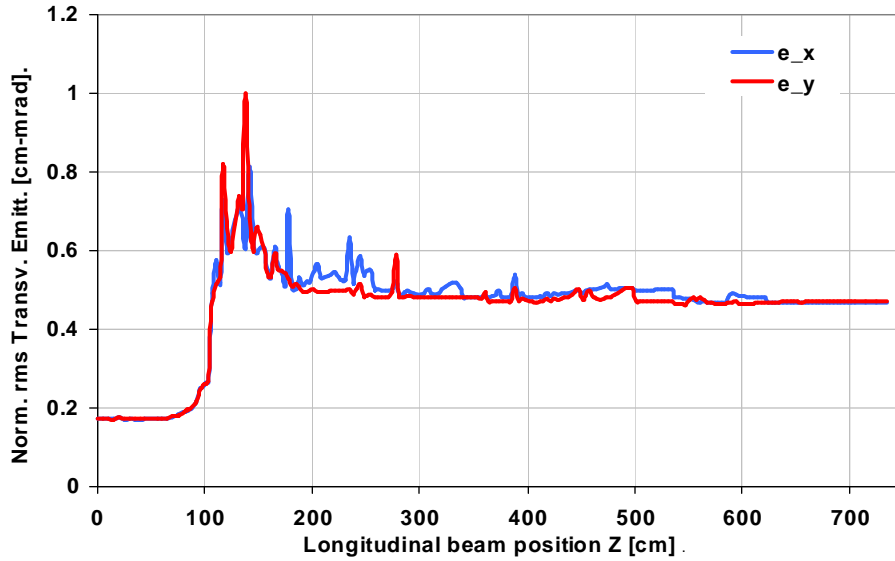


Fig. 4.4.12 Normalized transverse emittances evolution along the linac (top) and transverse phase plane distributions of 100 MeV beam (bottom).

4.4.4 Beam Diagnostics and Control

Beam diagnostics and control is one of the necessary systems to have good beam quality and beam parameters, which will correspond to the demand on the electron beam in the main linac. Beam diagnostic system in linac structure consists of BPMs (Beam Position Monitors (BPM), Faraday Cups (FC) and Optical Transition Radiation (OTR) detectors (Fig. 4.4.13).

The first FC is located just after the gun equipment. The location of the first FC will allow the beam current measurements at the gun exit, and to study the gun performance during the machine commissioning. The locations of BPMs are dictated by the need of information about beam position in the areas where the beam passes through one structure to another. With the control of the beam position along the linac, the beam trajectory will be corrected to meet design parameters of the beam according to linac specifications.

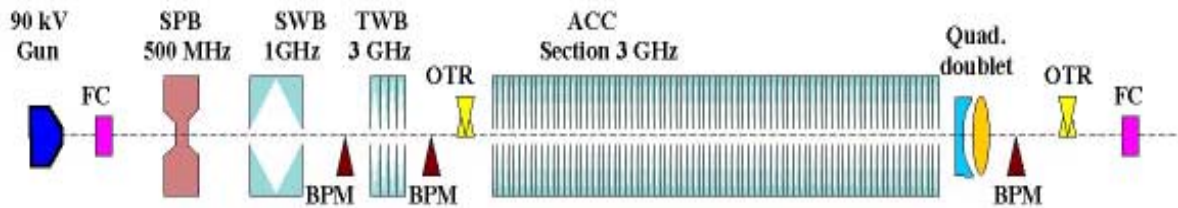


Fig. 4.4.13 Schematic layout of diagnostic elements for 100MeV main linac.

Two OTR detectors will be used to determine the beam transverse shape and energy spread before and after the main linear accelerating section. The data acquired by the first OTR detector will be used to tune-up the bunching section. The second OTR detector will perform the beam size measurements and in combination with the quadrupole doublet current variation will allow transverse emittance measurements. The OTR detector consists of a thin Al-foil that is almost transparent for electron beam.

The special software programs implemented into the control system will do the computation of transfer matrixes and the beamsize pictures analysis from the OTR monitors for the feedback system. The quantity and the names of the overall diagnostic devices used in linac are given in Table 4.4.6.

Table 4.4.6 The quantity of diagnostic device for linear injector.

Device name	Quantity
FC	2
OTR monitors	2
BPM	3
FS	2 or 3

The use of FS (Fluorescent Screens) mentioned in table is very optional. Their location will be defined during the design or prototype tests. The FS provides information about the beam image and can be useful for low beam current operation mode.

References

1. M. Schmitz “ The S-band Linear Collider Test Facility at DESY ”, for the SBLC study group, DESY, 1997.
2. M. Schmitz, “ Performance of the First Part of the Injector for S-band Test Facility at DESY ”, International Linac Conference, Switzerland, 1996.
3. E-GUN documentation, August 1992.
4. J.H. Billen, “PARMELA Documentation“, LA-UR-96-1835, revised February 2001.
5. “Handbook of Accelerator Physics and Engineering “, Editors: A. Chao, M. Tigner, World Scientific Publ. Co. Pte. Ltd. Singapore, 1999.
6. C. Travier, “RF Guns: review” Workshop on Short Pulse High Current Cathodes, France, June 1990.